applied optics

Method to calibrate a full-Stokes polarimeter based on variable retarders

Ivan Montes-González,* Neil C. Bruce, Oscar G. Rodríguez-Herrera, and Omar Rodríguez Núñez

Instituto de Ciencias Aplicadas y Tecnología, Universidad Nacional Autónoma de México, Ciudad Universitaria, Ciudad de México 04510, Mexico
**Corresponding author: ivan.montes@icat.unam.mx*

Received 25 March 2019; revised 13 May 2019; accepted 1 July 2019; posted 1 July 2019 (Doc. ID 363205); published 24 July 2019

We present a calibration method for a full-Stokes polarimeter. The polarimeter uses two liquid-crystal variable retarders (LCVR) and a linear polarizer to measure the four Stokes parameters. The calibration method proposed in this paper calculates the errors in the experimental setup by fitting the experimental intensity measurements for a set of calibration samples to a theoretical polarimeter with errors. The errors calculated in the method include the axes alignment errors and the errors in the retardance values of both LCVRs. The resulting calibration parameters are verified by measuring the polarization state of a light beam passing through a rotating linear polarizer, a half-wave plate, and a quarter-wave plate and comparing with the predictions for an ideal, error-free polarimeter. It is found that an average reduction in rms error of 55.8% can be obtained with the proposed method.

https://doi.org/10.1364/AO.58.005952

1. INTRODUCTION

The complete polarization state of a light beam may be represented by its Stokes vector, which describes all the polarization properties of an electromagnetic field and can be defined as [1–3]

$$S = \begin{pmatrix} S_0 \\ S_1 \\ S_2 \\ S_3 \end{pmatrix} = \begin{pmatrix} I_h + I_v \\ I_h - I_v \\ I_{45} - I_{-45} \\ I_{rc} - I_{lc} \end{pmatrix}, \quad (1)$$

where I_h, I_v, I_{45}, and I_{-45}, are the intensities of the horizontal, vertical, and 45° and −45° linear polarizations components, respectively. I_{rc} and I_{lc} are the intensities of the right and left circular polarization components.

A Stokes polarimeter allows us to determine the complete Stokes vector of a light beam, from intensity measurements. Polarimeters are widely used in many applications, such as remote sensing, medical diagnosis, or polarization microscopy [4–9], and some of these systems use liquid crystal variable retarders (LCVR) to manipulate the polarization state of a beam [10–12]. In our laboratory, we have characterized this type of retarder and found variations in the optical axis positions and retardance values [12–14]. These results show that we require better control of the LCVRs; in particular, temperature control and high-precision voltage control are necessary to stabilize the retardance values. However, these control systems are expensive, and we decided to search for improvements in the data-processing stage of Stokes polarimetry through the introduction of a calibration step.

In this paper, we propose a method to compensate errors in the angular positions of the axes and the induced retardance in the LCVRs. The Stokes polarimetry method used in this paper is based on a setup with two LCVRs and a linear polarizer. The application of at most six combinations of retardance values to the LCVRs and Eq. (1) is used to extract all the Stokes vector parameters from intensity data. The experimental setup, the theoretical analysis of the Stokes polarimeter, and the calibration method are shown in Section 2. Experimental results before and after the calibration are shown in Section 3. In Section 4, we present the conclusions.

2. EXPERIMENTAL SETUP AND THEORY

A. Stokes Polarimeter

The experimental setup for the Stokes polarimeter is shown in Fig. 1. For a light source, we used a 633 nm He–Ne laser, with a collimated beam spot of (0.837 ± 0.003) mm in diameter. The light passes through a beam splitter to yield an auxiliary beam to monitor and eliminate variations due to the laser instability. Then, the light passes through a linear polarizer to ensure that the incident light on the sample is polarized. After the sample, the light beam enters the Stokes polarimeter with a first LCVR, with its fast axis at 0°, a second LCVR, with its fast axis at 45°, and a horizontal linear polarizer, before entering the detector. The LCVRs used in this work are model

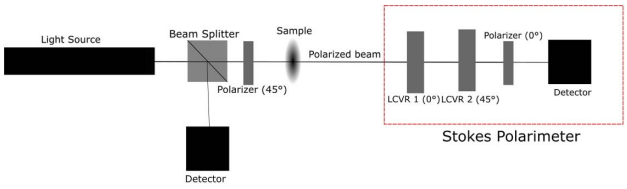

Fig. 1. Experimental setup for the Stokes polarimeter used in this work.

LCC2415-VIS by Thorlabs. Both detectors are model S120C, also by Thorlabs.

The Stokes vector entering the detector can be represented, using the Stokes–Mueller formalism in the following way:

$$S_D = \boldsymbol{M}_{P0}\boldsymbol{M}_{R2}\boldsymbol{M}_{R1}S_s = \boldsymbol{M}_{sys}S_s = \frac{1}{2}\begin{pmatrix} 1 & \cos\delta_2 & \sin\delta_1\sin\delta_2 & -\cos\delta_1\sin\delta_2 \\ 1 & \cos\delta_2 & \sin\delta_1\sin\delta_2 & -\cos\delta_1\sin\delta_2 \\ 0 & 0 & 0 & 0 \\ 0 & 0 & 0 & 0 \end{pmatrix} \times \begin{pmatrix} S_{s0} \\ S_{s1} \\ S_{s2} \\ S_{s3} \end{pmatrix} I_0, \tag{2}$$

where S_s is the Stokes vector of the light leaving the sample, $\boldsymbol{M}_{P0}$, $\boldsymbol{M}_{R2}$, and $\boldsymbol{M}_{R1}$, are the Mueller matrices of a horizontal linear polarizer, LCVR 2 and LCVR 1, respectively, and δ_i is the retardance value of LCVR i. The factor I_0 is a normalization factor depending on the incident intensity, which does not affect the measurements of the normalized Stokes parameters, and so will be dropped from the equations below. The first element of S_D is the total intensity of the light beam entering the detector and is the signal registered in the experiment. Performing the matrix multiplication in Eq. (2) and extracting only the first element of S_D, we find that the total, modulated intensity is given by

$$S_{D0} = \frac{1}{2}(S_{s0} + S_{s1}\cos\delta_2 + S_{s2}\sin\delta_1\sin\delta_2 - S_{s3}\cos\delta_1\sin\delta_2). \tag{3}$$

To calculate the complete Stokes vector, with four unknowns, at least four measurements must be made. However, according to Eq. (1), six intensity measurements are needed. In fact, Tyo showed that the optimum case, for which the measurement noise has a minimum effect on the final Stokes parameters, is for the condition number of the characteristic matrix of the polarimeter to be a minimum [15]. As shown by Tyo, the minimum condition number for a full Stokes polarimeter is $\sqrt{3}$, which is obtained for the case of the six independent intensity measurements given by Eq. (1). The characteristic matrix for this case is given by

Table 1. Retardance Values Used to Detect each Polarization Component

Combination	Detected Polarization	Retardance LCVR 1	Retardance LCVR 2
1	I_h	—	2π
2	I_v	—	3π
3	I_{45}	$\pi/2$	$\pi/2$
4	I_{-45}	$3\pi/2$	$\pi/2$
5	I_{rc}	2π	$\pi/2$
6	I_{lc}	π	$\pi/2$

$$A = \begin{pmatrix} 1 & 1 & 0 & 0 \\ 1 & -1 & 0 & 0 \\ 1 & 0 & 1 & 0 \\ 1 & 0 & -1 & 0 \\ 1 & 0 & 0 & 1 \\ 1 & 0 & 0 & -1 \end{pmatrix}, \tag{4}$$

and has a condition number of $\sqrt{3} = 1.732$. For the case of only four intensity measurements, the characteristic matrix is

$$A' = \begin{pmatrix} 1 & 1 & 0 & 0 \\ 1 & -1 & 0 & 0 \\ 1 & 0 & 1 & 0 \\ 1 & 0 & 0 & 1 \end{pmatrix}, \tag{5}$$

for which the condition number is not optimized and has a value of 3.2255. This case corresponds to horizontal, vertical, and +45° linear together with right circular polarization. In this work, we present and compare results for an optimized polarimeter, measuring six intensities, and a nonoptimized polarimeter, measuring only four intensities.

To retrieve the Stokes parameters, we measured the detected intensity for a combination of six retardance values for the first and second LCVR. As an example, to calculate I_h from Eq. (3), we set $\cos\delta_2 = 1$ and $\sin\delta_2 = 0$, which is true when $\delta_2 = 0, 2\pi, 4\pi, \ldots$ Hence, the measured intensity is

$$S_{D0} = \frac{1}{2}(S_{s0} + S_{s1}). \tag{6}$$

Using the relations in Eq. (1), the detected intensity is given by

$$S_{D0} = \frac{1}{2}(S_{s0} + S_{s1}) = \frac{1}{2}[(I_h + I_v) + (I_h - I_v)] = I_h. \tag{7}$$

Similar calculations will lead to the retardance values needed to measure the six polarization intensity components. These values are shown in Table 1. Notice that, in Table 1 there are two values for LCVR 1, which are not given. This is because these values have no effect on the detected intensity, so these values are arbitrary. In practice, we use the same value as given for Combination 3 in the table, to reduce the switching time between combinations. For the nonoptimized case, we use the same intensity values obtained in the optimized case, only selecting the four intensities required for the polarization states being analyzed.

B. Calibration Method

Calibration methods require an analysis of the results obtained with a number of known polarization calibration samples.

The detected intensities or the measured Stokes parameters are then compared with the ideal cases to deduce the errors in the system and the corrections required to obtain accurate results. In this paper, we propose the use of either four or six calibration samples; again, we compare the results of the two cases. As calibration samples, for the case of six samples we used a horizontal linear polarizer, a vertical linear polarizer, a half-wave retarder with its axes at 30° and at 60°, and a quarter-wave retarder with its fast axis at 30° and at 60°. These values of the axes angles of the fixed retarder plates were chosen to have contributions in as many as possible of the elements in the generated Stokes vectors. For the case of four calibration samples, we chose a horizontal linear polarizer, a vertical linear polarizer, a half-wave retarder with its fast axis at 30°, and a quarter-wave retarder with its fast axis at 30°. With these samples, in both cases we obtain contributions in the four Stokes parameters. Using an optimized polarimeter (six retardance combinations) and six calibration samples, we have 36 intensity measurements. With a nonoptimized polarimeter (four retardance combinations) and four calibration samples, we have only 16 intensity measurements. Obviously, this second case has the advantage of fewer measurements, which means a shorter measurement time. However, as shown below, there is an adverse effect on the final measurement precision.

The calibration procedure proposed consists of two stages. In the first stage, the experimental errors in the setup are calculated by fitting the experimental intensity measurements for the calibration samples to a theoretical polarimeter with errors. This is performed by using a nonlinear fitting procedure with the experimental errors as the fitting parameters and the sum of the differences between the experimental intensities and the calculated model intensities, including experimental errors, as the metric to be minimized. The measured intensities were fitted to the theoretical model with the error parameters using a computer program developed in our laboratory, along with the "Powell" algorithm [16]. Fitting algorithms need a starting solution, and we used an ideal experimental setup, without errors, as the starting value. The errors introduced in the polarimeter model to replicate the measured intensities were errors in each of the orientation angles of the LCVR axes and errors for each different value of the retardance of each LCVR. Other effects in the optical response of the LCVR, such as diattenuation and circular birefringence, were not considered in this model. This means that, for the optimized polarimeter (Table 1), there are four different retardance values for LCVR 1 and three different values of retardance for LCVR 2, giving a total of seven retardance errors. For the nonoptimized case, there are two retardance values for LCVR 1 and three for LCVR 2, giving a total of five retardance errors for this case. We also included errors in the axes positions of the calibration samples, giving one error for each sample. This means that the case of an optimized polarimeter and six calibration samples has 15 error terms, and so 15 fitting parameters in our method. For a nonoptimized polarimeter and only four calibration samples, we have a total of 11 fitting parameters. The metric, $\boldsymbol{M}$, used in the fitting procedure is the rms difference between the experimental and expected (theoretical) intensities over all the calibration samples and all of the polarimeter configurations:

$$\boldsymbol{M} = \left(\sum_{i=1}^{N} \sum_{j=1}^{n} \frac{1}{Nn} (S_{D0}^{\text{exp}} - S_{D0}^{\text{teo}})^2 \right)^{1/2}, \tag{8}$$

where the superscript exp denotes the experimentally measured intensity, the superscript teo denotes the theoretical intensity from the model of the polarimeter with errors, N indicates the number of calibration samples used (in our case, four or six), n denotes the number of intensities detected for each sample (again four or six), and this metric is minimized in the fitting procedure. The second step of the proposed method takes the fitting parameters optimized in the first step and assumes that they represent the fixed systematic experimental errors. Then, we use the intensity measurements of the unknown sample beam to obtain its complete Stokes vector, by fitting using the difference between the calculated and measured intensities as a metric, and the four Stokes parameters as the fitting parameters. In this case, we have four unknowns, the Stokes parameters, and either six intensities, for the optimized case, or four intensities, for the nonoptimized case. The metric, $\boldsymbol{M}'$, in this case is

$$\boldsymbol{M}' = \left(\sum_{j=1}^{n} \frac{1}{Nn} (S_{D0}^{\text{exp}} - S_{D0}^{\text{teo}})^2 \right)^{1/2}. \tag{9}$$

In this case, the superscript teo indicates the theoretical intensity using the polarimeter errors found in the first part of the fitting procedure and the theoretical values of the sample Stokes vector.

3. RESULTS

To verify the proposed method, we measured the Stokes parameters for three samples, i.e., a linear polarizer, a half-wave plate, and a quarter-wave plate, by rotating the axes of the samples from 0° to 180° in 10° increments. The Stokes parameters for the samples were calculated for ideal elements but include an error in the axis position for these samples. The calculated Stokes parameters were compared with the results obtained with our method, to verify our proposed method. With the rotation angle being given by θ, the theoretical Stokes vector are

$$S_{\text{pol}} = \begin{pmatrix} 1 \\ \cos(2\theta) \\ \sin(2\theta) \\ 0 \end{pmatrix}, \tag{10}$$

$$S_{\lambda/2} = \begin{pmatrix} 1 \\ \sin(4\theta) \\ -\cos(4\theta) \\ 0 \end{pmatrix}, \tag{11}$$

$$S_{\lambda/4} = \begin{pmatrix} 1 \\ \sin(2\theta)\cos(2\theta) \\ \sin^2(2\theta) \\ -\cos(2\theta) \end{pmatrix}. \tag{12}$$

Figures 2–4 show results obtained before and after applying the calibration method, for an optimized polarimeter with six calibration samples. The theoretical values are shown as styled

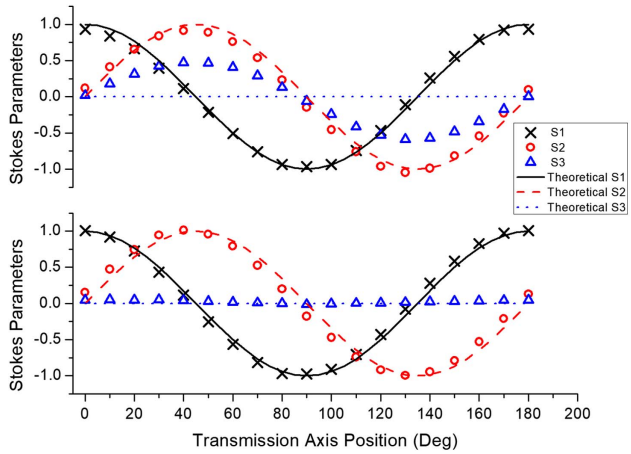

Fig. 2. Measured Stokes parameters (upper figure) and calibrated Stokes parameters (lower figure), for a rotating linear polarizer using an optimized polarimeter. Shaped points are the experimental values; styled lines are the theoretical values.

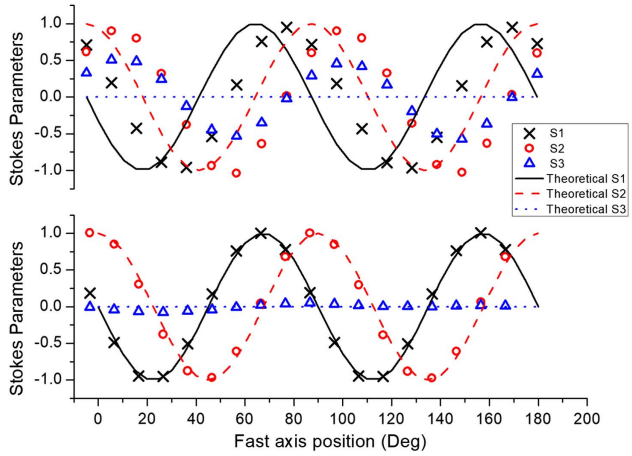

Fig. 3. As Fig. 2, but for a rotating half-wave plate.

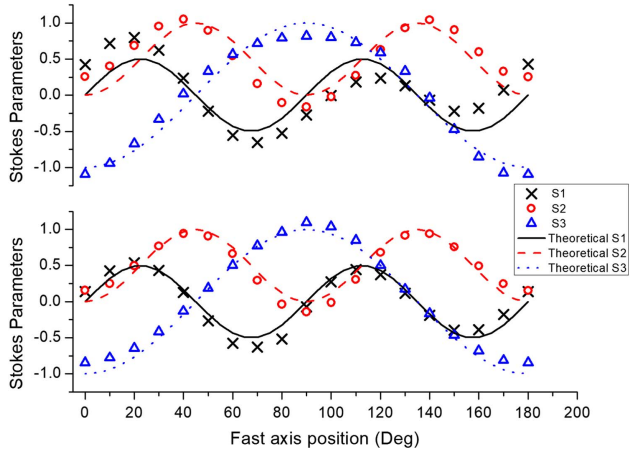

Fig. 4. As Fig. 2, but for a rotating quarter-wave plate.

lines without symbols and the experimental values as lines with shaped symbols.

From Figs. 2–4, it can be seen that there are large systematic errors in the uncalibrated results (upper graphs), particularly in the S3 terms in Figs. 2 and 3, as well as asymmetry in the S1 term of Fig. 4, which are mostly corrected by our proposed calibration procedure (lower graphs). The same type of measurements was made for an optimized and a nonoptimized polarimeter. The Stokes parameters obtained were compared with the theoretical values using Eqs. (6)–(8). We calculated the root mean square error (RMSE) for each Stokes parameter. The RMSE is defined as

$$\mathrm{RMSE} = \sqrt{\frac{1}{N_\theta}\sum_{n=1}^{N_\theta}\left(S_{Di}^{\mathrm{exp}} - S_{Di}^{\mathrm{theory}}\right)_n^2}, \tag{13}$$

where the subindex i indicates one particular Stokes vector element, the subindex n indicates the angle at which the Stokes vector is calculated, and there are N_θ rotation angles in the measurement of each Stokes vector. The values obtained directly from the experiment, with no calibration being performed, are shown in Fig. 5.

Figures 6 and 7 show the same results as Fig. 5 but calibrated with four and six calibration samples, respectively. After applying the calibration method, for an optimized polarimeter, the maximum RMSE is reduced by 48% and 51% using four and six calibration samples, respectively. For a nonoptimized polarimeter and using four calibration samples, the maximum RMSE increases, but using six samples the maximum RMSE is reduced by 30%. It can be seen that the calibration method proposed in this paper fails when it is used with a nonoptimized polarimeter and four calibration samples, having the best results when used with an optimized polarimeter and six calibration samples.

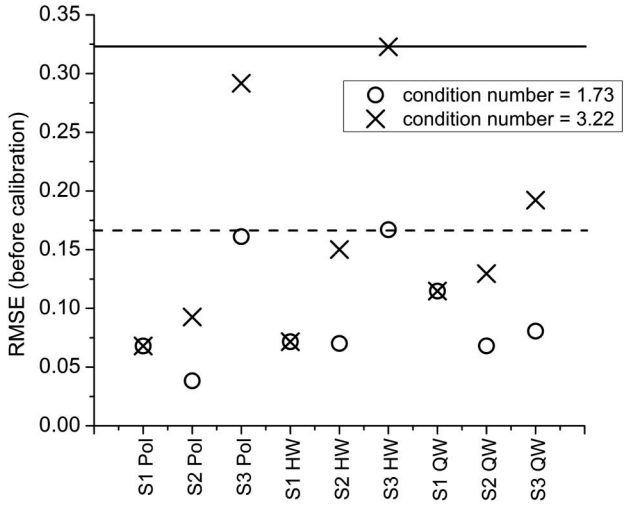

Fig. 5. RMSE in noncalibrated measured Stokes parameters with an optimized (circles) and nonoptimized polarimeter (crosses). Solid horizontal line marks the maximum RMSE (=0.3228) for a nonoptimized polarimeter and the dashed line the maximum (=0.1670) for an optimized polarimeter. The x axis indicates the element of the Stokes vector and the calibration sample used: Pol, linear polarizer; HW, half-wave retarder plate; QW, quarter-wave retarder plate.

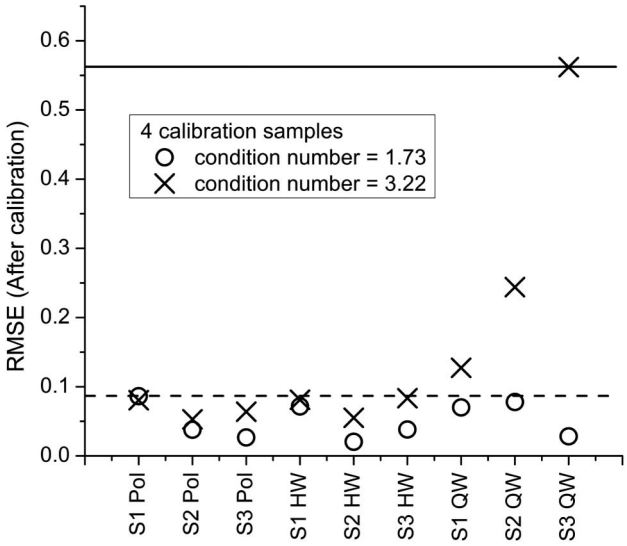

Fig. 6. RMSE in calibrated measured Stokes parameters with an optimized (circles) and nonoptimized polarimeter (crosses), using four samples in the calibration process. The solid horizontal line marks the maximum RMSE (=0.5610) for a nonoptimized polarimeter and the dashed line the maximum (=0.0864) for an optimized polarimeter. The *x* axis indicates the element of the Stokes vector and the calibration sample used: Pol, linear polarizer; HW, half-wave retarder plate; QW, quarter-wave retarder plate.

We made three sets of nine Stokes parameter measurements using an optimized polarimeter and six calibration samples. But, before each measurement, the LCVRs were recharacterized, the experimental setup was reassembled, and the calibration samples were measured. The calibration calculation was applied each time we measured the complete Stokes vector of the three rotating samples. These test runs show the stability of the experimental setup and of the calibration method proposed. The results of these measurements are shown in Fig. 8.

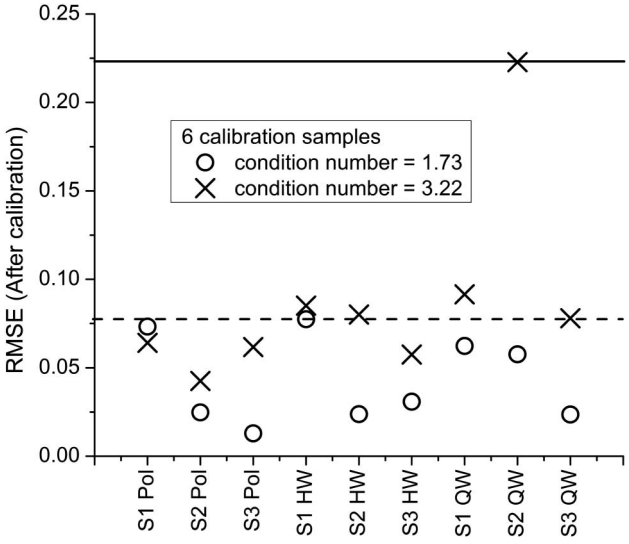

Fig. 7. RMSE in calibrated measured Stokes parameters with an optimized (circles) and nonoptimized polarimeter (crosses), using six samples in the calibration process. The solid horizontal line marks the maximum RMSE (=0.2228) for a nonoptimized polarimeter and the dashed line the maximum (=0.0774) for an optimized polarimeter. The *x* axis indicates the element of the Stokes vector and the calibration sample used: Pol, linear polarizer; HW, half-wave retarder plate; QW, quarter-wave retarder plate.

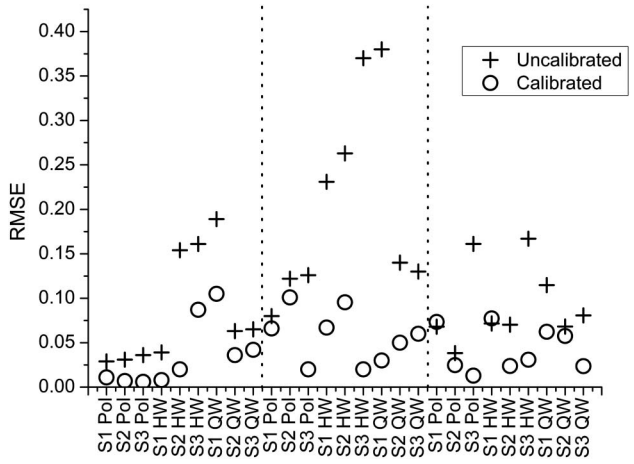

Fig. 8. RMSE of measured Stokes parameters, before (crosses) and after (circles) applying the calibration method, using six calibration samples, with an optimized polarimeter. The *x* axis indicates the element of the Stokes vector and the calibration sample used. Vertical dotted lines separate the different test runs performed.

In Fig. 8, we can see that the precision of the final results changes with alterations in the experimental system. However, with the calibration process proposed here, nearly all of the RMSE after the calibration are less than those before the calibration. There are two values of RMSE in the third test run that have a larger RMSE after calibration, but the absolute value of the changes in RMSE is small (in the third decimal place) for both cases. The worst case RMSE after the calibration is 0.105, and the RMSE is reduced by the calibration between 17% and 94.5%. The average reduction of the RMSE for all the cases is 55.8%. Figure 9 shows the percentage reduction in

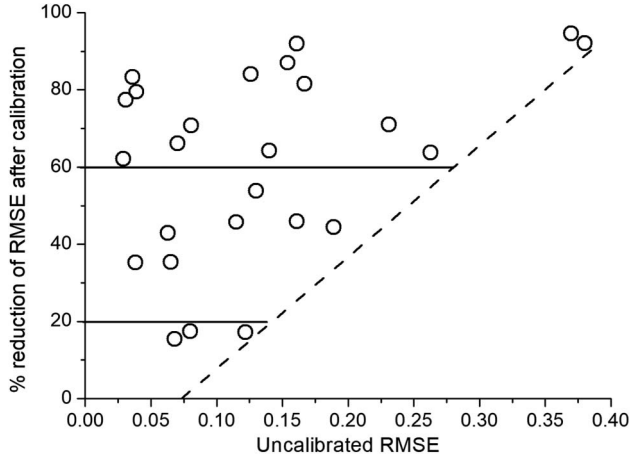

Fig. 9. Percentage reduction of the RMSE as a function of uncalibrated RMSE, showing that higher values of the uncalibrated RMSE tend to have a higher correction percentage. Dotted line is drawn as an aid for visualization of the tendency.

the RMSE with our calibration procedure as a function of the uncalibrated RMSE. This figure shows that most of the measurements have reductions above 60% for any value of the uncalibrated RMSE. All values below 20% of reduction of the RMSE appear for uncalibrated RMSE values that are already lower than about 0.12. This figure also shows that higher values of the uncalibrated RMSE tend to have larger percentage reductions in the calibrated RMSE, as shown by the dashed line drawn on the graph as an aid to visualization.

4. CONCLUSIONS

A method to calibrate Stokes polarimeters has been presented. It is based on fitting the intensity measurements of calibration samples to the intensities obtained using a theoretical polarimeter with errors. The experimental errors in the polarimeter, including the retardance values for the LCVRs and the axes position of the LCVRs and calibration samples, are taken into account by this method. We applied the method to measurements with a Stokes polarimeter using two liquid-crystal variable retarders, which we have found to have variations in their output due to voltage-dependent rotations in their fast axes, variations in the applied voltage, and the well-known temperature dependence of the induced retardance.

Experimental data for an optimized polarimeter and six calibration samples yield good results, having a reduction of up to 94.5% in the RMSE after the calibration. The results for a nonoptimized polarimeter and/or only four calibration samples are also improved using the proposed calibration method, although these improvements were not as important as for the case of an optimized polarimeter and six calibration samples. Although the analysis was performed for only two condition numbers, the results are clear and show that this method can help to reduce errors in the measurements of the Stokes vectors.

Funding. Dirección General de Asuntos del Personal Académico, Universidad Nacional Autónoma de México (DGAPA, UNAM) (PAPIIT IT100417, PAPIIT TA100219).

Acknowledgment. Ivan Montes-González and Omar Rodríguez-Núñez thank CONACYT for the doctoral scholarship received.

REFERENCES

1. D. Goldstein, *Polarized Light* (CRC Press, 2003).
2. R. A. Chipman, *Handbook of Optics* (McGraw-Hill, 1995), Chap. 22.
3. W. S. Bickel and W. M. Bailey, "Stokes vectors, Mueller matrices and polarized scattered light," Am. J. Phys. **53**, 468–478 (1985).
4. F. Liu, X. Shao, and P. Han, "Design of a circular polarization imager for contrast enhancement in rainy conditions," Appl. Opt. **55**, 9242–9249 (2016).
5. J. S. Tyo, D. L. Goldstein, D. B. Chenault, and J. A. Shaw, "Review of passive imaging polarimetry for remote sensing applications," Appl. Opt. **45**, 5453–5469 (2006).
6. D. Miller and E. Dereniak, "Selective polarization imager for contrast enhancements in remote scattering media," Appl. Opt. **51**, 4092–4102 (2012).
7. D. Louie, L. Tchvialeva, S. Kalia, H. Lui, and T. Lee, "One-shot Stokes polarimetry for low-cost skin cancer detection," Proc. SPIE **10869**, 1086904 (2019).
8. J. Zhou, H. He, Y. Wang, and H. Ma, "Stage scoring of liver fibrosis using Mueller matrix microscope," Proc. SPIE **10024**, 100240M (2017).
9. A. Le Gratiet, M. Dubreuil, S. Rivet, and Y. Le Grand, "Scanning Mueller polarimetric microscopy," Opt. Lett. **41**, 4336–4339 (2016).
10. A. de Martino, Y.-K. Kim, E. García-Caurel, B. Laude, and B. Drévillon, "Optimized Mueller polarimeter with liquid crystals," Opt. Lett. **28**, 616–618 (2003).
11. A. Peinado, A. Lizana, J. Vidal, C. Iemmi, and J. Campos, "Optimization and performance criteria of a Stokes polarimeter based on two variable retarders," Opt. Express **18**, 9815–9830 (2010).
12. J. M. López-Téllez and N. C. Bruce, "Stokes polarimetry using analysis of the nonlinear voltage-retardance relationship for liquid-crystal variable retarders," Rev. Sci. Instrum. **85**, 033104 (2014).
13. J. M. López-Téllez, N. C. Bruce, and O. G. Rodríguez-Herrera, "Characterization of optical polarization properties for liquid crystal-based retarders," Appl. Opt. **55**, 6025–6033 (2016).
14. I. Montes-Gonzalez, N. C. Bruce, and J. M. Lopez-Tellez, "Polarization characterization of liquid-crystal variable retarders," Proc. SPIE **9960**, 996014 (2014).
15. J. S. Tyo, "Design of optimal polarimeters: maximization of signal to noise ratio and minimization of systematic errors," Appl. Opt. **41**, 619–630 (2002).
16. W. H. Press, S. A. Teukolsky, W. T. Vetterling, and B. P. Flannery, *Numerical Recipes in C: The Art of Scientific Computing* (Cambridge University, 1992).